5'-AMP-activated protein kinase alpha regulates stress granule biogenesis

Hicham Mahboubi, Ramla Barisé, and Ursula Stochaj

Department of Physiology McGill University, 3655 Promenade Sir William Osler, Montreal, PQ, H3G 1Y6, Canada.

*Corresponding author: Ursula Stochaj
Phone: 514-398-2949; Fax: 514-398-7452; E-mail: ursula.stochaj@mcgill.ca

Abbreviations. AMPK, 5'-AMP-activated protein kinase; CC, compound C; DAPI, 4', 6-diamidino-2-phenylindole; ECL, enhanced chemiluminescence; FBS, fetal bovine serum; FRET, fluorescence resonance energy transfer; KD, knockdown; PBS, phosphate-buffered saline; PLA, proximity ligation assay; SG, stress granule.

Highlights

1. AMPK-α2 is a *bona fide* component of cytoplasmic stress granules
2. AMPK-α controls the biogenesis of cytoplasmic stress granules
3. AMPK-α2 binds directly to the granule nucleation protein G3BP1 in stress granules
4. Stress stimulates the interaction between AMPK-α2 and G3BP1

Abstract

Stress granule (SG) assembly represents a conserved eukaryotic defense strategy against various insults. Although essential for the ability to cope with deleterious conditions, the signaling pathways controlling SG formation are not fully understood. The energy sensor AMP-activated protein kinase (AMPK) is critical for the cellular stress response. Human cells produce two AMPK catalytic α-subunits with partially overlapping, but also unique functions. Here, we provide direct support for structural and functional links between AMPK-α isoforms and SGs. As such, several stressors promote SG association of AMPK-α2, but not AMPK-α1. Multiple lines of evidence link AMPK activity to SG biogenesis. First, pharmacological kinase inhibition interfered with SG formation. Second, AMPK-α knockdown combined with in-depth quantitative SG analysis revealed isoform-specific changes of SG characteristics. Third, overexpression of mutant α-subunits further substantiated that AMPK regulates SG parameters. Finally, we identified the SG-nucleating protein G3BP1 as an AMPK-α2 binding partner. This interaction is stimulated by stress and notably occurs in SGs. Collectively, our data define the master metabolic regulator AMPK as a novel SG constituent that also controls their biogenesis.

Keywords: 5'-AMP-activated protein kinase; stress granules; signaling; oxidative stress; apoptosis; quantitative microscopy.

1. Introduction

Eukaryotic cells have evolved different strategies to control energy expenditure and survival during environmental or physiological stress. One of the main mechanisms is stress granule (SG) formation in the cytoplasm, where SGs store translationally arrested mRNAs that are associated with a diverse set of proteins and protect cells from apoptosis [1, 2]. SG biogenesis is a conserved stress response; in most cases, SG assembly is induced by phosphorylation of the translation initiation factor eIF2α. This results in polysome disassembly, translation arrest and subsequent SG formation [3, 4]. However, SGs can also form independently of eIF2α phosphorylation [5, 6]. SG nucleation is initiated by the oligomerization of G3BP1 (Ras GTPase-activating protein-binding protein 1 and aggregation of prion-like domains of the RNA binding proteins TIA-1/TIAR [7, 8]. Secondary recruitment of additional proteins produces mature SGs [9], which vary in RNA and protein composition according to the type of stress [4, 10, 11].

Recent studies have begun to decipher the signaling events that control SG formation. For example, focal adhesion kinase (FAK) is recruited to SGs and regulates SG dynamics during the recovery from stress [12]. RhoA and the downstream kinase ROCK1 also associate with SGs and are involved in their assembly [13]. At the same time, SG formation can also control intracellular signaling and cell fate. For example, RACK1 sequestration in SGs inhibits apoptosis-inducing p38 and JNK pathways and thus favors cell survival [1]. In addition, the energy sensing mTOR pathway regulates cell survival through the SG recruitment of Raptor [14]. Thus, SGs are important signaling hubs that control key cellular decisions [2, 15]. However, the signaling pathways regulating SG biogenesis are far from being fully understood.

One of the stress responsive kinases is AMPK, a central regulator of energy homeostasis in eukaryotes [16, 17]. When cellular ATP pools are depleted, the kinase is activated; as a result, cells shift from anabolic to catabolic processes ([18]; reviewed in [19]). AMPK impinges on numerous cell functions, ranging from autophagy, cell growth and polarity to cytoskeletal dynamics [20-24].

The heterotrimeric AMPK (αβγ) contains one catalytic α subunit which is encoded by two genes (α1 and α2). The regulatory β and γ subunits are encoded by two and three genes, respectively [25]. The role of AMPK as a key regulator of metabolism requires a tight control of the enzyme [26-29]. The most important step for AMPK activation is the phosphorylation of its α-subunit on Thr183 (human α1) or Thr172 (human α2), a modification catalyzed by several upstream kinases [30].

Interestingly, the two α-isoforms have overlapping as well as unique functions. For instance, both AMPK-α1 and AMPK-α2 reduce cell death upon metabolic stress, and the two subunits can substitute for each other [31]. Isoform-specific functions for AMPK-α2 include the regulation of transcription and tumor survival in high grade gliomas, while AMPK-α1 modulates the neurotoxicity of Huntington's disease [32, 33]. Moreover, AMPK-α1 activation causes a nucleocytoplasmic redistribution of TDP43, a SG protein that is linked to neurodegenerative disorders [34, 35].

Here, we defined the role of AMPK for SG biogenesis and identified α-isoform-specific contributions to this process. To our knowledge, our studies are the first to demonstrate a direct link between AMPK and SG biogenesis.

2. Materials and methods

2.1. Cell culture, stress and drug treatment

HeLa cells were grown in Dulbecco's modified eagle medium (DMEM) containing antibiotics and 8% Fetal Bovine Serum (FBS). Cultures were maintained in a 37°C incubator containing 5% CO_2. To induce oxidative stress, HeLa cells were treated with 0.5mM sodium arsenite or sterile water (control) for 1h. Alternatively, HeLa cells were incubated with 2mM diethyl maleate (DEM) or ethanol (control) for 4h. For treatment with compound C (CC), cells were pre-incubated for 1h with DMSO (vehicle) or 40μM CC and subsequently incubated with ethanol or DEM; DMSO or CC was present throughout the stress exposure. For energy depletion, 10mM sodium azide was combined with 50mM 2-deoxyglucose (NDG); cells were treated for 30min and controls were incubated with water. To induce SGs independent of eIF2α phosphorylation [36], HeLa cells were exposed for 30min to 0.1μM Pateamine A (generously provided by Drs. Gallouzi and Pelletier).

2.2. Indirect immunofluorescence

Cells were grown to 70% confluency on poly-lysine coated cover slips. After treatment, immunofluorescent staining was performed following published procedures [37]. Antibody dilutions were: AMPK-α1/2 (1:200; Santa Cruz sc-74461), AMPK-α1 and AMPK-α2 (1:2000; Bethyl A300-507A, A300-508A), AMPK-β1/2 (1:400; Cell Signaling #4150), AMPK-γ1 (1:200; Cell Signaling #4187), AMPK-γ2 (1:200; Cell Signaling #2536), HuR (1:2000; sc-5261), TIA-1/TIAR (1:1000; sc-28237), G3BP1 (1:1000; BD Biosciences #611126), myc-epitope (1:1,000; sc-40). In brief, cells were fixed with 3.7% formaldehyde in phosphate-buffered saline (PBS), permeabilized with 0.1% Triton X-100 in PBS/2mg/BSA and blocked for 1h in PBS containing 5% FBS, 0.05% Tween-20 and 1mM NaN_3. Samples were incubated overnight with primary antibodies diluted in PBS/FBS/Tween. Purified Alexa Fluor®488, Alexa Fluor®647 and Cy3 fluorescently-labeled secondary antibodies were added the following day for 2h [38]. Nuclei were visualized with 1μg/ml 4', 6-diamidino-2-phenylindole (DAPI). The specificity of primary antibodies against AMPK subunits and SG marker proteins was evaluated (Suppl. Fig. 1, [38] and [39]). Cover slips were mounted on glass slides and images acquired in the multi-track mode with a Zeiss LSM510 confocal microscope. Appropriate filter settings were chosen to minimize cross-talk between channels. Images were processed in Adobe Photoshop 8.0. 3D reconstruction and surface rendering were performed with Imaris software (Bitplane) on confocal stacks acquired with 0.35μm intervals.

2.3. Gene silencing

FastFect (Feldan) was used to transfect HeLa cells with shRNA plasmids according to the manufacturer's protocol. Transfected cells were identified by co-transfection of a plasmid encoding the fluorescent protein mCherry. Two sequences targeting different regions of the AMPK-α1 or α2 genes were used for each knockdown (Table S1); the control shRNA-construct contained a scrambled sequence. All sequences were blasted against the human genome to verify appropriate target recognition. After a 3-day knockdown period cells were exposed to stress and analyzed.

2.4. Transfection of plasmid DNA

Plasmid DNA was introduced into HeLa cells with FastFect as recommended by the manufacturer. All constructs contained a pcDNA3.1 backbone and encoded a myc-tagged protein. The myc-tag was used to identify transfected cells. The K45R AMPK-α2 mutant (provided by Dr. M. Birnbaum [40]) codes for a kinase-dead protein and is dominant negative. A constitutively active AMPK-α2 mutant with T172D substitution was generated by site-specific mutagenesis; the correctness of the construct was verified by DNA sequencing. A plasmid encoding a C-terminal fragment of DNAJA2 (gift from J. Young, McGill University) produces an inactive protein and served as control [41]. 24h after transfection, cells were incubated with oxidant or vehicle and then processed for immunofluorescence.

2.5. Image quantification

SGs were quantified with MetaXpress software according to our published procedures [11]. In brief, individual cells were identified based on the staining with DAPI and the transfection marker. Following background correction, SG parameters were measured using G3BP1 as a marker for the compartment. All steps were recorded in a custom-designed journal to automate the quantification.

2.6. Cell death assessment

Nuclear fragmentation of DAPI-stained fixed and mounted cells was scored to evaluate cell death.

2.7. Cell extracts

HeLa cell proteins were solubilized in gel sample buffer as described [42]. Samples were incubated at 95ºC for 10min and vortexed with silica beads to shear DNA. Proteins were precipitated with trichloroacetic acid for 20min on ice and collected by centrifugation (microfuge, 1 min at 13000 rpm). Sediments were resuspended in gel sample buffer and analyzed by Western blotting.

2.8. Western blotting

Western blotting and ECL followed standard procedures. Primary antibodies were used at the following dilutions: AMPK-α1/2 (1:200), p-AMPK-α (1:2000; Cell Signaling #2535), p-Acc1 (1:1000; phosphoSer79; Cell Signaling #3661); Acc1 (1:500; Cell Signaling #3662), HuR (1:2000), G3BP1 (1:2000), TIA-1/TIAR (1:1000), AMPK-α1 and AMPK-α2 (1:2000), actin (1:100,000; Chemicon). Primary antibodies were detected with HRP-conjugated secondary antibodies.

2.9. Proximity ligation assay (PLA)

PLA was performed with the Duolink II kit (Olink Bioscience), essentially as recommended by the manufacturer. In brief, samples were fixed, permeabilized, blocked and incubated with primary antibodies as described above. Samples were then washed with blocking buffer and incubated for 1h at 37ºC with secondary antibodies conjugated with PLA probes. After two washes with buffer A (Olink Bioscience), the ligation was performed for 30min at 37ºC, followed

by amplification (100min at 37ºC) and final washes with buffer B. After completing all PLA steps, Alexa Fluor®488 conjugated secondary antibodies were added for 2h at room temperature, samples were washed in blocking buffer, incubated with DAPI and mounted.

2.10. Co-immunoprecipitation

Reversible protein crosslinking with Dithiobis (succinimidyl propionate) and immunoprecipitation were essentially as described [43]. In brief, after incubation with DEM or vehicle, crosslinking was carried out for 15min at room temperature. Samples were rinsed with PBS and 50mM Tris HCl pH 7.4/150mM NaCl and stored at -70ºC. For immunoprecipitation, cell extracts were incubated overnight at 4ºC with 1.5µg anti-G3BP1 or non-specific mouse IgG. Protein G-Sepharose was then added for 2h at 4ºC. The resin was washed, bound material separated on 7.5-10% acrylamide gradient gels and analyzed by Western blotting [43]. Filters were probed with anti-G3BP1 antibodies, stripped and reprobed with anti-AMPK-α2. Bound AMPK-α2 antibodies were detected with HRP-conjugated secondary antibodies specific for rabbit IgG light chains (Jackson Labs., #211-032-171). ECL signals were quantified, and the ratio AMPK-α2/G3BP1 was calculated. Results were normalized to the control sample.

2.11. Statistics

At least three independent experiments were performed for each assay/condition and One-way ANOVA analysis was carried out to identify significant differences**;** * $p<0.05$; ** $p<0.01$. Results for co-immunoprecipitation are shown for four independent experiments; data for controls and treated samples were compared by Student's ttest.

3. Results and discussion

3.1. Oxidative stress targets AMPK to SGs

Under normal growth conditions, AMPK resides in the nucleus or cytoplasm, shuttling between the two compartments [37]. Stressors that promote SG formation also alter the intracellular AMPK distribution. These conditions increase AMPK concentrations in nuclei [37]; the fate of cytoplasmic kinase pools, however, is not well defined.

To address this point, HeLa cells were incubated with the oxidant diethyl maleate (DEM), a compound that induces SGs [11]. In DEM-treated cells, AMPK-α1/2 associated in the cytoplasm with granular compartments that colocalized with the SG markers G3BP1 and HuR (Fig. 1A). (Suppl. Fig. 1 verified the specificity of AMPK antibodies used for our studies.)

Since the SG composition depends on the type of stress, we also evaluated sodium arsenite, an oxidant frequently used to produce SGs. As for DEM, AMPK-α1/2 located to SGs in arsenite-treated cells (Fig. 1B).

3.2 AMPK-α isoforms are differentially recruited to SGs

To identify the catalytic subunit(s) associated with SGs, we immunostained stressed cells with isoform-specific antibodies. AMPK-α2 was present in all SGs induced by DEM or arsenite (Fig. 2). By contrast, AMPK-α1 was detected only in few SGs of DEM-treated cells; these SGs were

particularly large. This isoform-dependent distribution of AMPK-α subunits was verified with different isoform-specific primary antibodies (Fig. 2, Fig. 1 in [39]). Furthermore, we confirmed these findings in another cell type from a distinct organism (mouse embryonic fibroblasts, Fig. 2 in [39]). As AMPK is a heterotrimeric enzyme that contains β and γ subunits, we also assessed the presence of these regulatory proteins in SGs (Fig. 3-5 in [39]). In parallel, control experiments evaluated the non-specific staining with secondary antibodies alone. Following oxidative stress, β-subunits associated with SGs (Fig. 3 in [39]). While SG staining was not observed for the γ1 subunit (Fig. 4 in [39]), γ2 was detected in the SGs produced upon DEM treatment and in large arsenite-induced SGs (Fig. 5 in [39]). Since *PRKAG3*, the gene encoding AMPK γ3, is predominantly expressed in muscle [44], we did not include the γ3 subunit in our studies. Future experiments will have to undertake a comprehensive assessment of how regulatory AMPK subunits interact with SGs.

3.3. AMPK-α2 associates with SGs that are generated by metabolic stress or Pateamine A

Experiments in Fig. 2 demonstrated that oxidants promote the SG association of AMPK-α2. To characterize further the SG recruitment of AMPK, we exposed cells to metabolic stress caused by energy-depletion. As observed for oxidants, AMPK-α2, but not AMPK-α1, was detected in SGs after the combined treatment with sodium azide and 2-deoxyglucose (Fig. 3).
Under many conditions, SG formation is stimulated by the phosphorylation of eIF2α on Ser51. While this modification is not mandatory to produce SGs, SGs assembled in the absence of eIF2α phosphorylation can differ in their composition [6]. The translation inhibitor Pateamine A induces SGs without promoting Ser51 phosphorylation of eIF2α [36]. In HeLa cells, SGs assembled upon Pateamine A incubation contained the marker proteins HuR and G3BP1, as well as AMPKα (Fig. 4). Like other stressors, AMPKα binding was isoform-specific; AMPK-α2, but not AMPK-α1, associated with SGs produced by Pateamine A (Fig. 4).
Taken together, upon oxidative, metabolic or drug-induced stress, SGs are assembled that contain AMPK-α2, but not AMPK-α1. In addition to the catalytic α2 subunit, some regulatory AMPK subunits also located to SGs. This establishes AMPK-α2 as a *bona fide* SG component in different cell types and organisms. Notably, AMPK-α2 is recruited to SGs induced by eIF2α phosphorylation-dependent and -independent pathways. This supports the idea that AMPK-α2 controls SG formation for a wide variety of stress conditions.

3.4. The enzymatic activity of AMPK is required for proper SG formation

To examine the role of AMPK activity for SGs, we blocked its kinase activity with the pharmacological inhibitor compound C [CC, [45]]. Immunofluorescence studies and Western blotting showed that the phosphorylation of AMPK-α1/2 and its downstream target Acc1 were greatly reduced by the inhibitor (Fig. 5A-C). Treatment with CC diminished the size of oxidant-induced SGs as revealed by the marker proteins HuR and G3BP1 (Fig. 5A, B). Notably, AMPK inhibition did not prevent its recruitment to SGs. While SGs were smaller in CC-treated cells, they still contained AMPK-α (Fig. 5A). We observed the same outcome with sodium arsenite (Fig. 3B), suggesting that independent of the type of oxidant AMPK is required to produce mature SGs. In line with the presence of SGs in CC-treated cells, the compound did not prevent the phosphorylation of eIF2α upon oxidative stress (Fig. 5C). Furthermore, no profound changes were caused by CC for the concentrations of SG core proteins TIA-1/TIAR, G3BP1 or HuR.

These data support a model proposing that the enzymatic activity of AMPK is required to assemble SGs of normal size. However, AMPK is not essential to promote the stress-induced phosphorylation of eIF2α and the initial steps of SG assembly. Accordingly, AMPK is likely to control the growth of SGs.
Others reported recently that CC reduces the size of SGs that were generated upon cold shock [46]. However, direct evidence that implicates AMPK in SG assembly is missing. The following section imparts this information. Moreover, it identifies the specific SG parameters that are regulated by AMPK.

3.5. AMPK-α isoform-specific regulation of SGs

Although CC is commonly used to inhibit AMPK, the agent has off-target effects [47-49]. A shRNA silencing approach will provide independent and direct evidence to substantiate the role of AMPK for SG formation. To this end, two different constructs were generated for each of the two α-subunits. Isoform-specific antibodies verified the knockdown efficiency of all constructs by Western blotting (Fig. 6A). Notably, depletion of the AMPK-α1 subunit increased significantly AMPK-α2 protein levels, indicating a compensatory mechanism to restore AMPK activity. By contrast, AMPK-α2 knockdown also reduced AMPK-α1 protein levels, and this was the case for two different shRNA constructs (Fig. 6A). Our results confirm previous observations that knockdown strategies which specifically target AMPK-α2 efficiently diminish AMPK-α1 concentrations [50]. Together with other publications ([51] and references therein), our data demonstrate a complex regulatory interplay between the two α-subunits that has to be dissected in the future.
We further assessed the impact of α1- or α2-knockdown on DEM-induced SGs. In these experiments, mCherry identified cells transfected with the silencing construct (Table S1); SGs were then demarcated with G3BP1 (Fig. 6B). G3BP1 presents a robust SG marker for our studies, because AMPK-α knockdown did not significantly alter G3BP1 concentrations (Fig. 6 in [39]).
To evaluate SG formation in an unbiased fashion, multiple granule parameters were quantified with our established protocols [11]. These measurements were performed for individual cells or SGs. On the single cell level, the number of SGs/cell and the total SG area/cell were determined, while the SG area was calculated for individual granules. Our methods also inform on the SG composition as it relates to G3BP1. Specifically, the pixel intensity for G3BP1/SG area reflects the G3BP1 content of the granule.
The comprehensive analyses depicted in Fig. 5C revealed that targeting AMPK-α2 for knockdown reduced three SG parameters, the number of SGs/cell, the total SG area/cell and the SG pixel intensity. The pixel intensity/SG area remained unchanged, indicating that α2-subunit depletion did not significantly alter the G3BP1 content. Unlike AMPK-α2, the α1-specific knockdown did not affect any of the SG characteristics assessed (Fig. 6C). Similar results were obtained for each of the two α-subunits with two different shRNA constructs (sh1, sh2). In ethanol-treated control cells no major changes were observed.
Taken together, we established for the first time that AMPK depletion impairs the formation of mature SGs. Our measurements of SG parameters identified AMPK as a novel regulator that controls several SG characteristics. Moreover, we uncovered α-isoform-specific differences that implicate AMPK-α2 in SG assembly. It is noteworthy that AMPK-α2 knockdown diminished both α-subunits. It is therefore possible that AMPK-α2 depletion alone or the concomitant loss of

both α-subunits altered SG characteristics. While our data do not distinguish between these possibilities, they nevertheless show the importance of AMPK-α2 for SG biogenesis.

3.6. AMPK depletion diminishes cell survival in stressed cells

SGs regulate the survival of stressed cells; it was therefore possible that AMPK knockdown alters cell viability under oxidative stress conditions. To address this point, we scored cell death based on the nuclear morphology, according to established criteria [52]. AMPK-α knockdown cells were examined in the absence or presence of oxidant. Under stress, both AMPK-α1 and AMPK-α2 were required for cell survival, as the percentage of cells with fragmented nuclei increased significantly for all knockdown experiments (Fig. 7). AMPK-α2 knockdown somewhat increased cell death in ethanol-treated cells, albeit not significantly. Thus, our results indicate that both α-isoforms contribute to cell survival in response to stress. As discussed above, AMPK-α2 knockdown may elevate cell death due to the loss of AMPK-α2, AMPK-α1 or both. Since nuclear fragmentation was similar for all AMPK-α knockdown experiments, it is likely that cell death was not primarily due to changes in SG assembly. It is conceivable that the small SGs produced after AMPK-α2 knockdown can still prevent extensive cell death.

3.7. AMPK knockdown does not alter the levels of core SG proteins

TIA-1/TIAR, G3BP1 and HuR represent core SG proteins; TIA-1/TIAR and G3BP1 are especially important, because they nucleate SGs [7]. As discussed above, CC treatment did not change the levels of these core SG proteins (Fig. 5C). Similarly, no substantial differences were detected upon knockdown of AMPK-α1 or AMPK-α2 (Fig. 6 in [39]). Our results support the model that the AMPK-mediated effects on SGs are downstream of the steps that initiate granule assembly. In this scenario, AMPK is critical to the generation of mature SGs.

3.8. A dominant-negative AMPK-α2 mutant reduces the number of SGs

Our results for CC and AMPK-α2 knockdown are consistent with the idea that the enzymatic activity of AMPK is critical for the formation of proper SGs. To further test this hypothesis, we transiently transfected HeLa cells with myc-tagged AMPK-α2 variants that were dominant negative (K45R) or constitutively active (T172D). Control cells produced a biologically inactive myc-tagged form of DNAJA2 [41]. Transfected cells were identified with antibodies against the myc-tag, and SG parameters were quantified for cells treated with DEM or the vehicle ethanol (Fig. 8). The dominant negative AMPK-α2 mutant did not prevent the stress-induced assembly of SGs, but led to a significant reduction of the number of SGs/cell and the total SG area/cell. On the other hand, constitutive AMPK activation somewhat increased the SG area, but these changes were not significant. Upon transfection some SGs were also induced in vehicle-treated cells; there was no significant difference between the various plasmids introduced (Fig. 8, EtOH).
Collectively, these results corroborate our CC and knockdown studies and link AMPK activity to SG biogenesis. Our data also show that AMPK activation in the absence of stress is not sufficient to induce SG assembly, a conclusion supported by pharmacological AMPK activation (data not shown).

3.9. AMPK-α2 physically interacts with G3BP1 in SGs

Experiments described above demonstrate that AMPK-α2 locates to SGs, but binding partners in the granules are unknown. To begin to define the interaction network of AMPK-α2 that is related to SG components, we performed *in situ* proximity ligation assays (PLA) with the core SG protein G3BP1 as a candidate interactor. G3BP1 and AMPK-α2 were in close proximity in SGs (Fig. 9), and additional interactions occurred in the cytoplasm, but outside of SGs (Fig. 9A, C). The PLA signals were specific, because negative controls missing one of the primary antibodies gave no or only weak signals. To verify that our protocol is appropriate for the detection of protein-protein interactions in SGs, we reproduced the association between HuR and TIA (Fig. 9B). FRET studies showed previously that HuR and TIA interact in SGs [53].
AMPK-α2 binding to the resident SG protein G3BP1 could promote SG growth through several not mutually exclusive mechanisms. Since G3BP1 shuttles in and out of SGs [54] it could provide a carrier that targets AMPK-α2 to the granules. Interestingly, we detected interactions between AMPK-α2 and G3BP1 in the cytoplasm, but outside of SGs (Fig. 9A, C). These associations could represent an initial contact that is followed by the movement to SGs. In an alternative scenario, AMPK-α2 may phosphorylate G3BP1 in SGs, and thereby promote SG maturation through the recruitment of other SG components. Without AMPK-α2, G3BP1 will still locate to SGs, but the formation of full-size granules will be prevented.

3.10. Oxidative stress regulates the interaction between AMPK-α2 and G3BP1

The PLA experiments in Fig. 9 established that AMPK-α2 interacts with G3BP1 in SGs. We further characterized this interaction by co-immunoprecipitation experiments in control and DEM-treated cells (Fig. 10). Immunoprecipitation of G3BP1 co-purified AMPK-α2, while nonspecific binding to isotype control IgG was low. The major AMPK-α2 band obtained after co-immunoprecipitation was a protein of ~50kD apparent molecular mass. By contrast, this band was not purified with control IgG. As the starting material contained little or none of the ~50kD band, it likely represents AMPK-α2 that was cleaved during the process of immunoprecipitation. To determine whether the interaction between AMPK-α2 and G3BP1 was controlled by stress we calculated the ratio AMPK-α2/G3BP1 in immunoprecipitates. These measurements showed a significant increase of AMPK-α2 binding under stress conditions (Fig. 10). Thus, we provided independent evidence for the presence of AMPK-α2 and G3BP1 in the same protein complexes. The formation of these complexes occurs under non-stress conditions, but is significantly increased when cells produce SGs. Our results provide independent evidence that further substantiates the model proposed in the previous section. Moreover, it is possible that SGs serve as a platform that stimulates the interaction between AMPK-α2 and G3BP1.

3.11. How is AMPK activation linked to SG biogenesis?

CC experiments, AMPK-α2 knockdown and the overexpression of a dominant-negative AMPK-α2 mutant are consistent with the idea that the enzymatic activity of AMPK controls SG assembly. On the other hand, 4h incubation with DEM reduces the phosphorylation of the α-subunits on Thr183/Thr172 [37]. To resolve this apparent inconsistency, we determined the kinetics of AMPK activation and SG formation during DEM treatment. At early time points (5-20min) Thr172/Thr183 phosphorylation transiently increases (Fig. 11), and SGs were detected after 1h of treatment. Likewise, a transient AMPK activation was also described for arsenite [55].

Collectively, these data support the interpretation that a transient spike in AMPK activity is a prerequisite for proper SG maturation.

4. Conclusions

Taken together, we have linked AMPK directly to a hallmark of the stress response, the assembly of SGs. Our results are summarized in the simplified model depicted in Fig. 12. In particular, we demonstrated the isoform-specific presence of AMPK in SGs, where the kinase interacts with G3BP1. Based on these results, we propose that AMPK is part of an intracellular signaling hub that is located in SGs.

In line with AMPK's function as a stress sensor, SG formation preserves energy under detrimental growth conditions [2]. We now present, for the first time, evidence that these two key regulators of cellular energy homeostasis are directly linked. Given the dynamic properties of AMPK and the growing number of substrates modified by the enzyme, our report sets the stage to explore new directions to fully understand the physiological roles of AMPK and its isoforms. This applies in particular to cells exposed to environmental stress or diseases that are linked to the production of SGs and related granules.

Acknowledgements

This work was supported by grants from NSERC, FQRNT and HSFC. HM is a recipient of a doctoral fellowship from NSERC. We are grateful to Drs. M. Birnbaum (University of Pennsylvania), I. Gallouzi, R. Jones, J. Orlowski, J. Pelletier and J. C. Young (McGill University) for their generous gift of reagents.

Figures and figure legends.

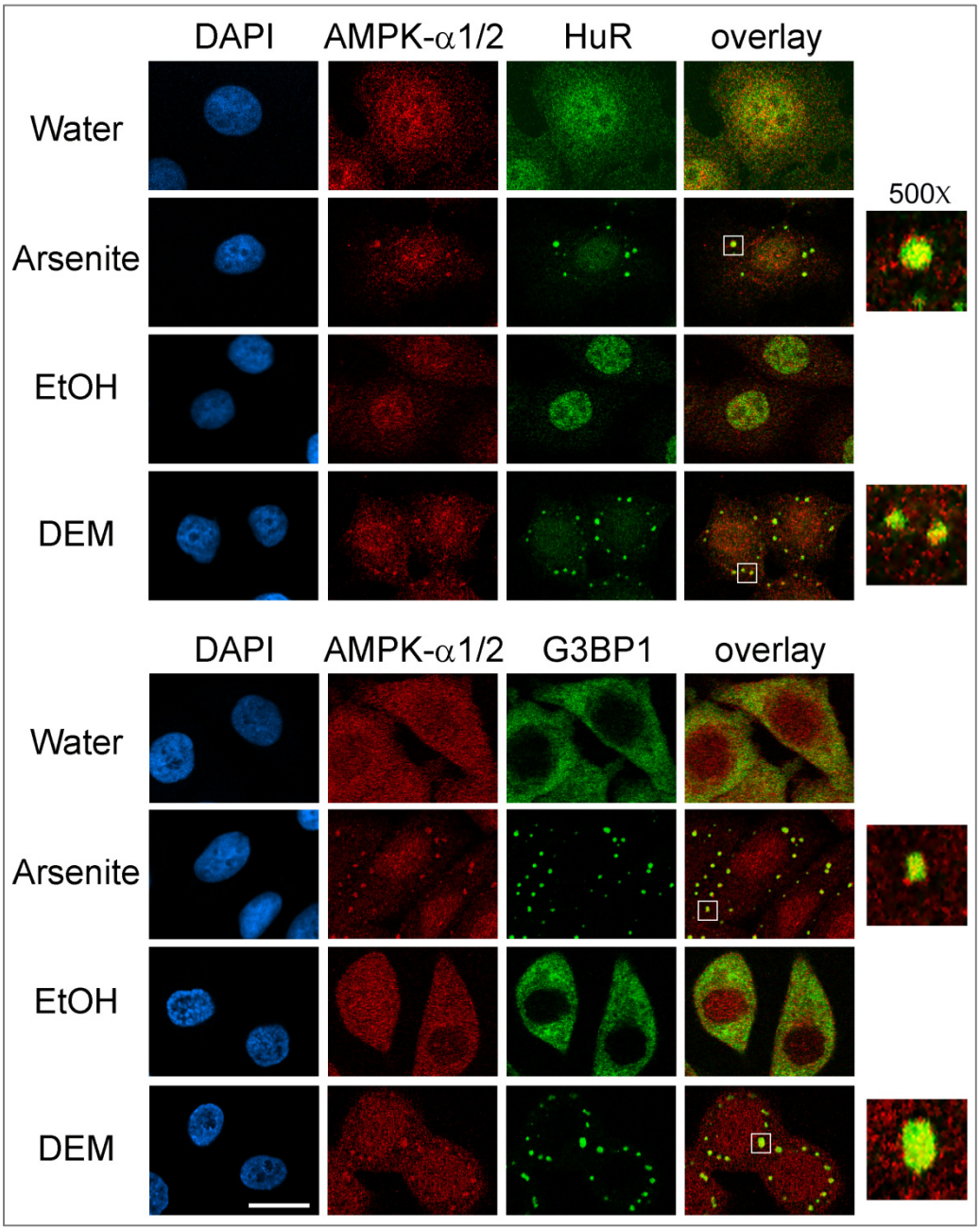

Fig. 1. AMPK-α1/2 localizes to SGs in response to oxidative stress. HeLa cells were incubated with the vehicle water or ethanol, and SG formation was induced with arsenite or DEM (Materials and methods). Antibodies against AMPK-α1/2 recognize both isoforms of the α-subunit. A portion of AMPK-α1/2 associated with SGs which were identified with the marker proteins HuR or G3BP1. DNA was visualized with DAPI. Magnified (500X) sections show the co-localization of AMPK-α with the SG marker protein in the overlay. Scale bar is 20µm.

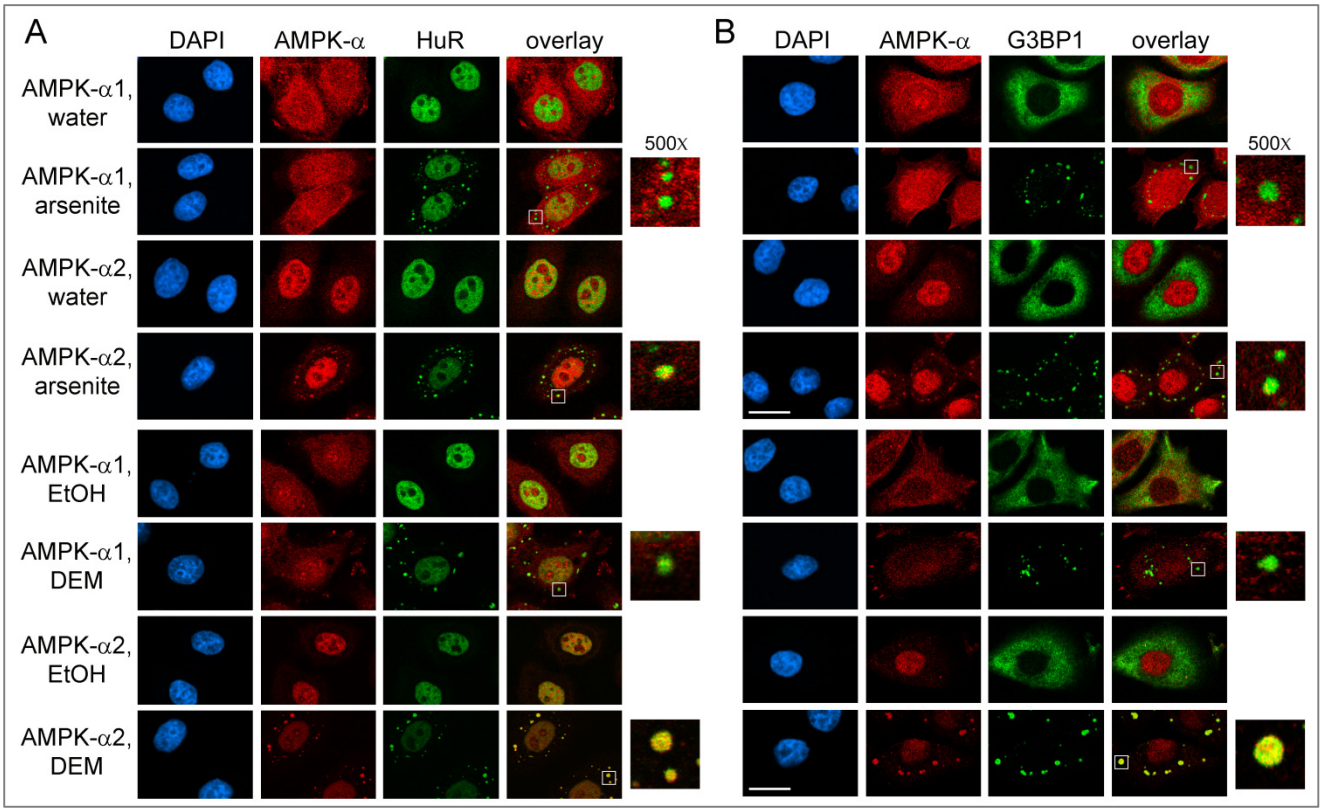

Fig. 2. AMPK-α isoforms are differentially recruited to SGs. Cells were treated as described for Fig. 1 and incubated with antibodies specific for AMPK-α1 or AMPK-α2. AMPK-α2 was present in SGs induced by arsenite or DEM. By contrast, little or no SG staining was observed for AMPK-α1. (A) SGs were identified with HuR; (B) SGs were demarcated with G3BP1. Selected SGs were magnified (500X) to show the colocalization (yellow) of AMPK-α with SG marker proteins. Scale bar is 20μm.

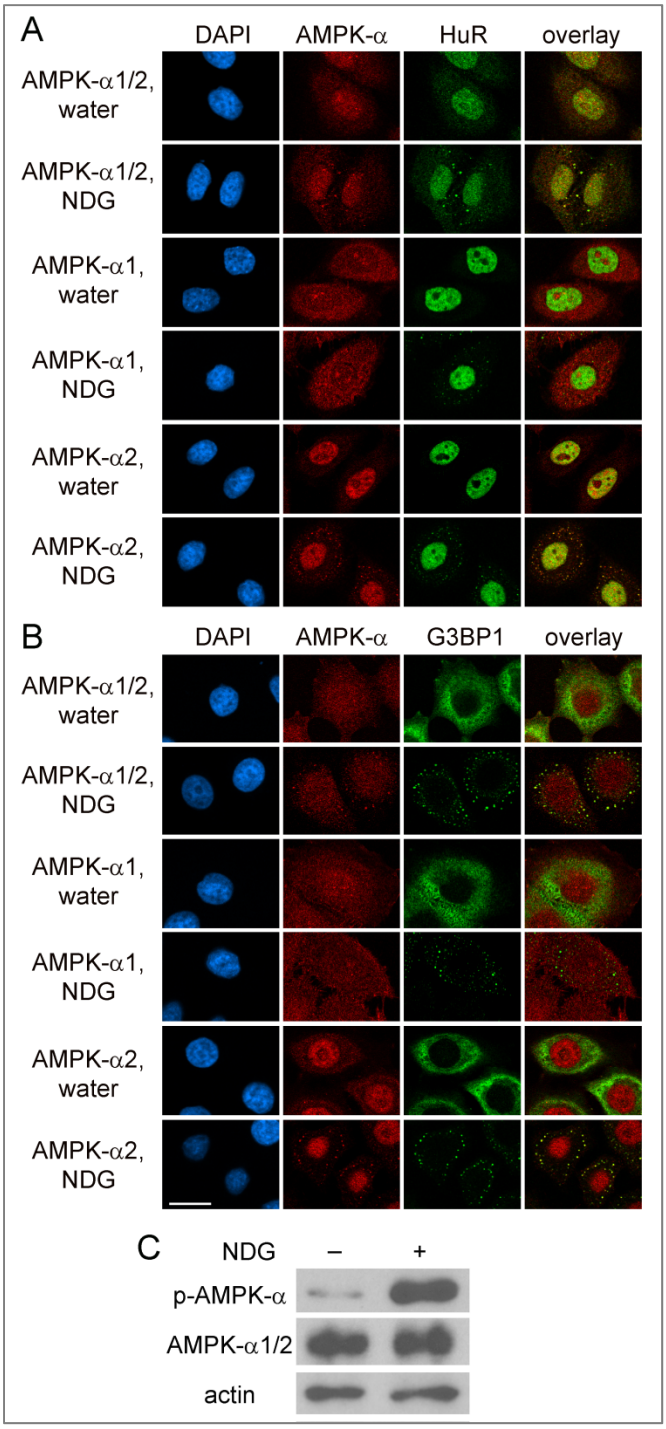

Fig. 3. Energy depletion induces SG assembly and activates AMPK. HeLa cells were energy depleted with sodium azide and 2-deoxyglucose (NDG). (A, B) Fixed cells were analyzed by indirect immunofluorescence with antibodies against AMPK-α1, AMPK-α2, HuR (part A) or G3BP1 (part B), as indicated. Scale bar is 20μm. (C) Western blotting confirmed the increased phosphorylation of AMPK-α in energy-depleted cells.

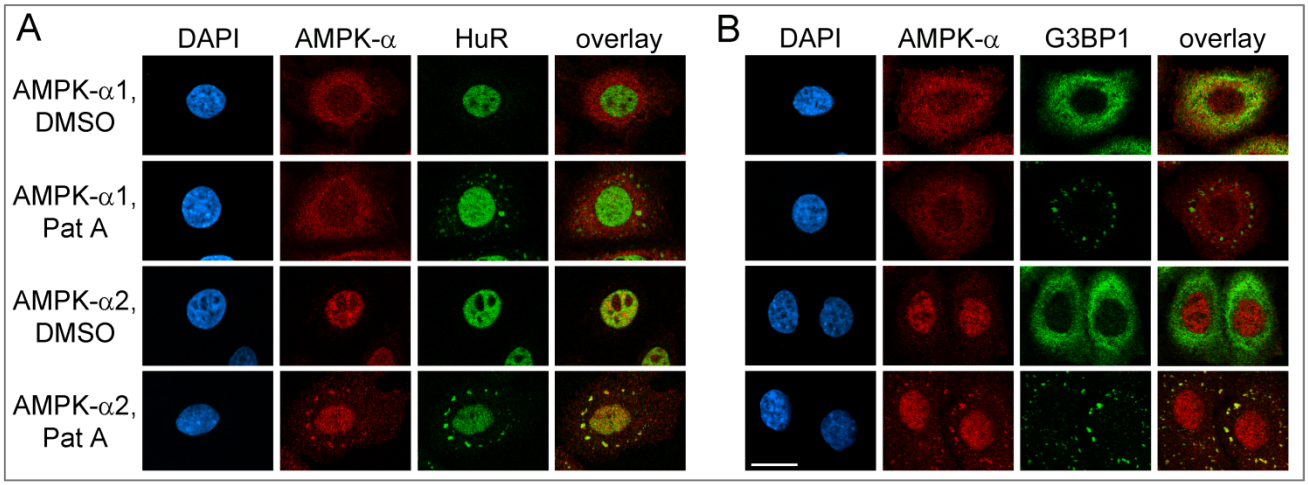

Fig. 4. AMPK-α2 is recruited to SGs that form independent of eIF2α phosphorylation. HeLa cells were incubated with vehicle DMSO or Pateamine A (PatA) and then processed for the immunodetection of (A) AMPK-α and HuR, or (B) AMPK-α and G3BP1. Scale bar is 20µm, nuclei were stained with DAPI.

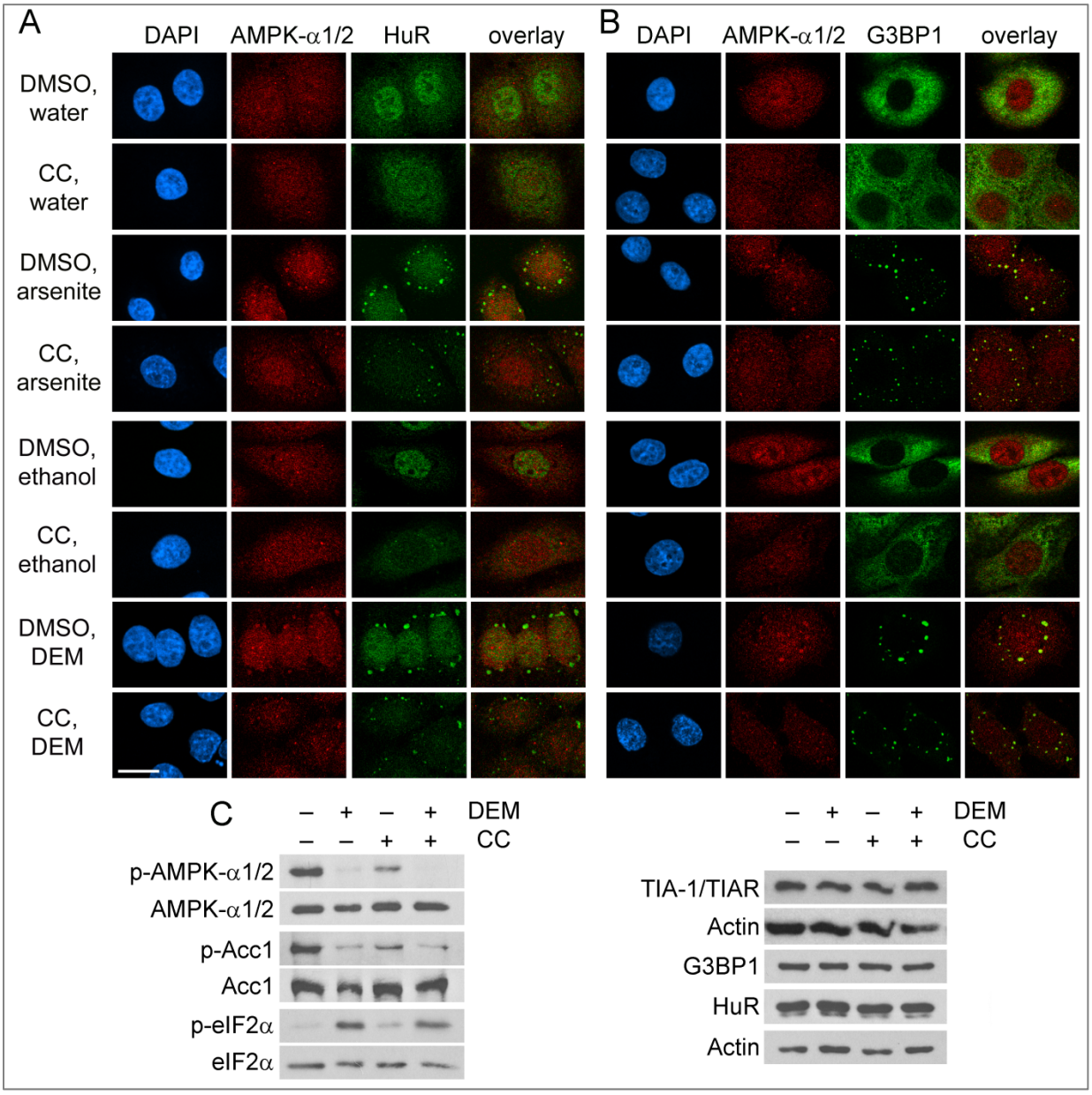

Fig. 5. Compound C impairs SG formation. (A) HeLa cells were pre-incubated with the vehicle DMSO or CC for 1h; DMSO or CC was also present throughout the subsequent treatment period. SG assembly was induced by arsenite; the vehicle water was added to controls. Alternatively, SGs were produced with DEM, whereas controls received ethanol. AMPK-α1/2 was detected in SGs demarcated with the marker HuR. (B) The same results as in part A were obtained with the SG marker G3BP1. Scale bar is 20µm. (C) Western blots for control and DEM-treated samples show a reduction of α-subunit phosphorylation (α1, Thr183; α2, Thr172) after DEM incubation. CC further diminishes this modification. The loss of AMPK kinase activity was verified by probing for phosphorylated Acc1 (p-Acc1). Phosphorylation of eIF2α on Ser51 was not abolished by DEM or CC. DEM or CC had also no strong effects on the cellular concentrations of TIA-1/TIAR, G3BP1 or HuR.

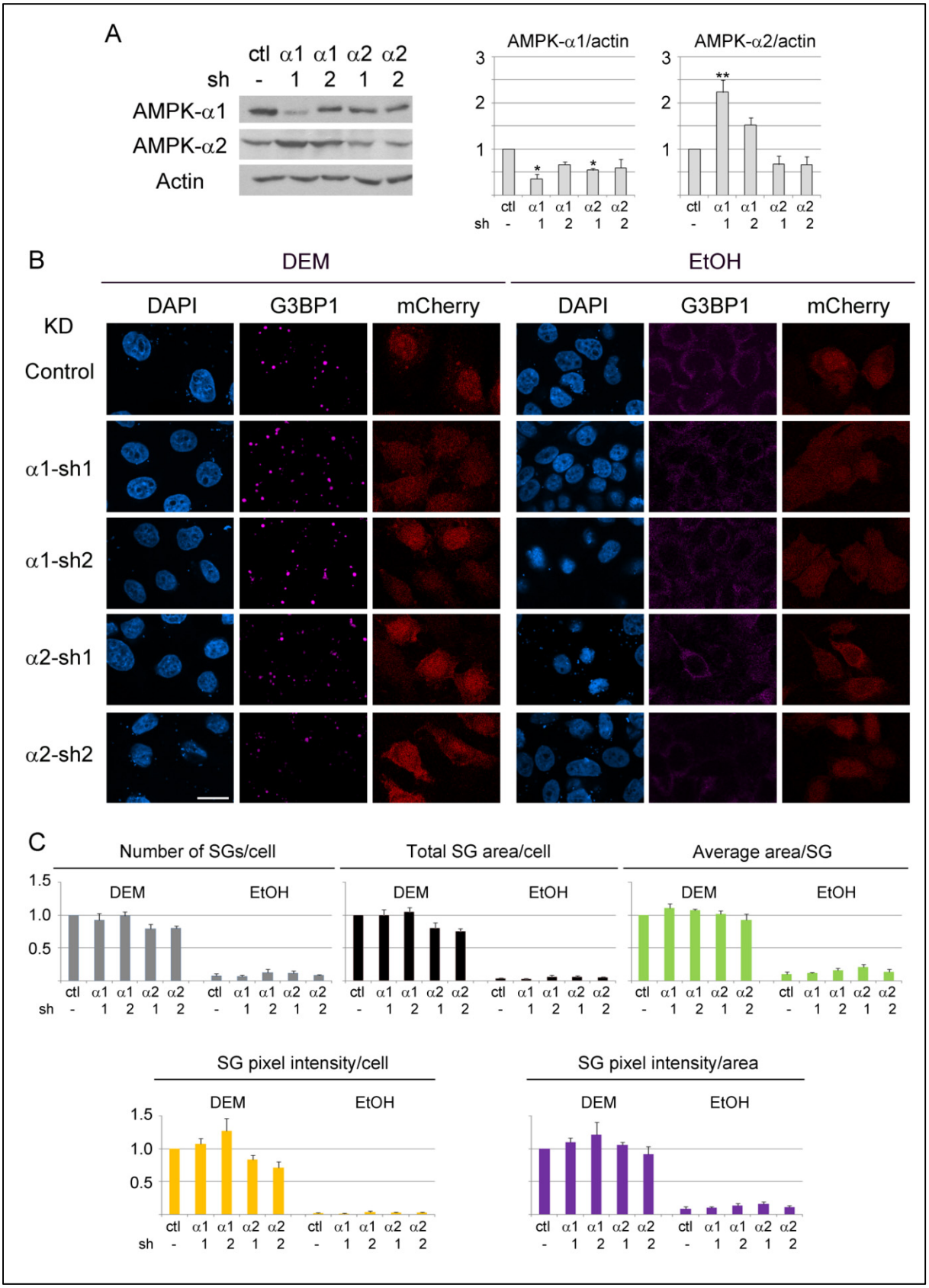
A
ctl α1 α1 α2 α2
sh - 1 2 1 2
AMPK-α1
AMPK-α2
Actin
AMPK-α1/actin
AMPK-α2/actin
B
DEM
EtOH
DAPI
G3BP1
mCherry
KD
Control
α1-sh1
α1-sh2
α2-sh1
α2-sh2
C
Number of SGs/cell
Total SG area/cell
Average area/SG
SG pixel intensity/cell
SG pixel intensity/area

Fig. 6. AMPK-α knockdown has isoform-specific effects on SGs. The impact of AMPK-α1 or AMPK-α2 knockdown was assessed in cultured cells. (A) Isoform-specific knockdown was analyzed by quantitative Western blotting. Note that AMPK-α1 knockdown upregulates the concentration of AMPK-α2, whereas AMPK-α2 knockdown also diminishes the α1-isoform levels. Similar results were obtained for two different constructs targeting each isoform. Results are shown as average +SEM for three independent experiments. (B) Cells knocked down for AMPK-α isoforms were identified with the transfection marker mCherry. SGs in DEM- or ethanol-treated cells were demarcated with G3BP1. Scale bar is 20µm. (C) SG parameters were quantified for three independent experiments. AMPK-α2 knockdown reduced the number of SGs/cell, the total SG area/cell and the SG pixel intensity/cell.

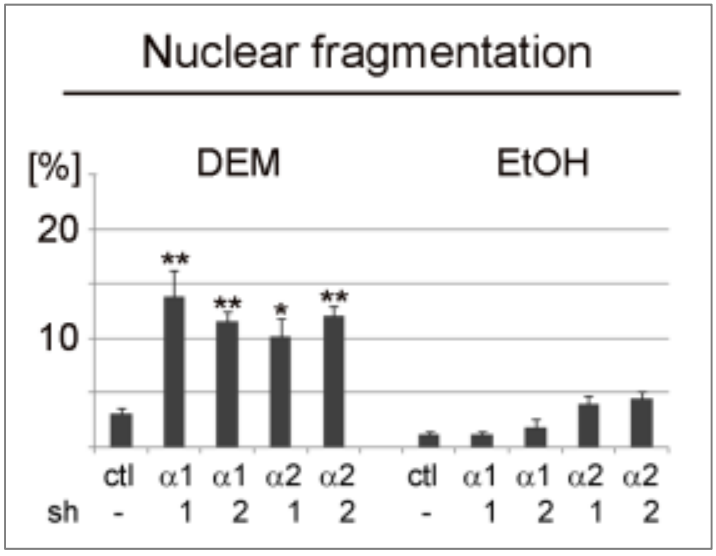

Fig. 7. AMPK-α1 or AMPK-α2 knockdown significantly increases the number of cells with nuclear fragmentation, indicating cell death. One-way ANOVA identified significant changes for all quantitative measurements; * $p<0.05$; ** $p<0.01$.

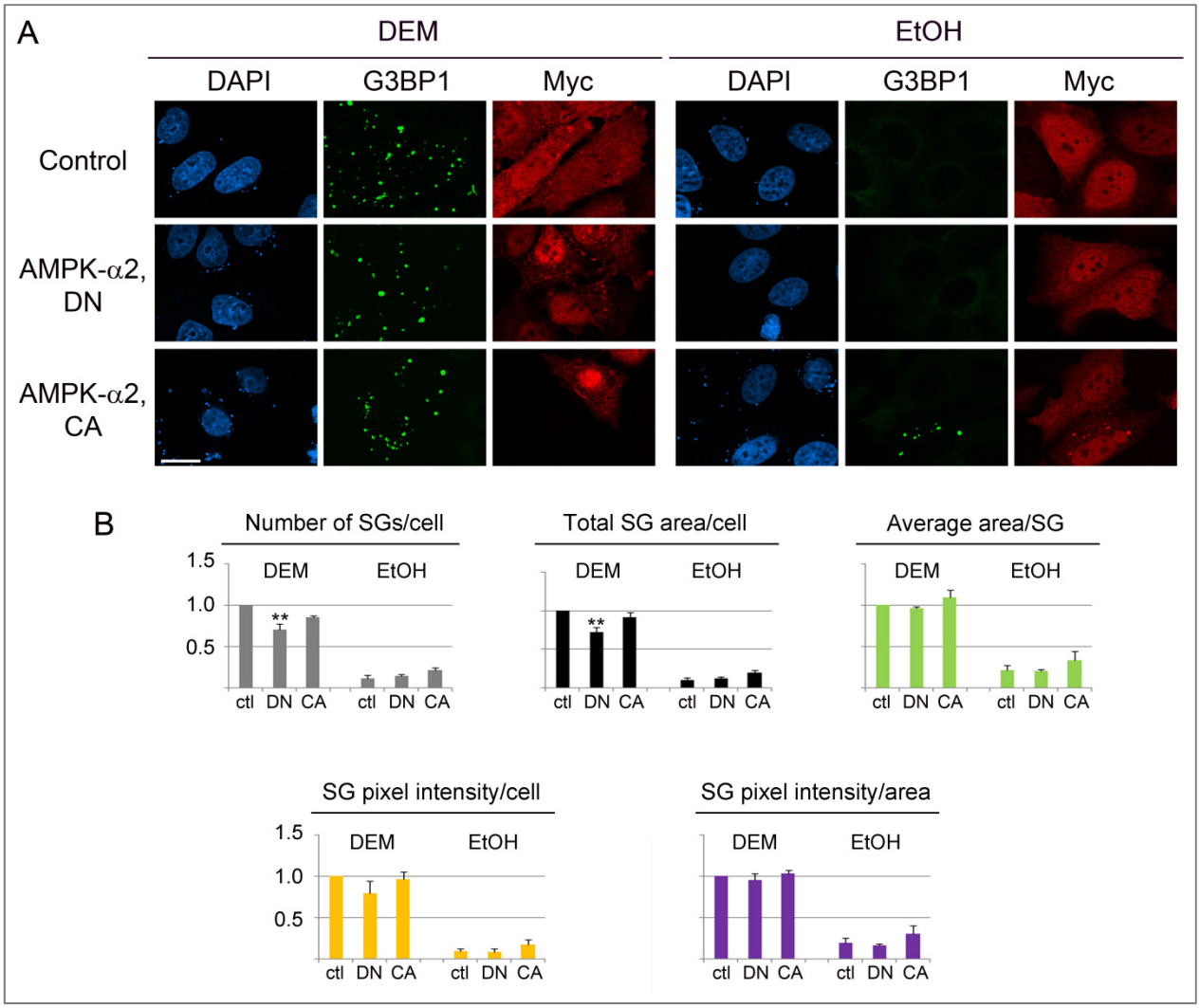

Fig. 8. A dominant-negative mutant of AMPK-α2 changes SG parameters. HeLa cells were transiently transfected with control DNA, or plasmids encoding a dominant-negative (DN) or constitutively active (CA) form of AMPK-α2. Cells were exposed to DEM or the vehicle ethanol (EtOH), fixed and analyzed by quantitative immunofluorescence. (A) The SG marker G3BP1 and myc-tagged proteins were detected; all images were acquired and processed with identical settings. Scale bar is 20µm, nuclei were demarcated with DAPI. (B) Different SG parameters were quantified as described for Fig. 6. Results are shown for three independent experiments; at least 63 cells were quantified per experiment for each plasmid. Results were normalized to the control DNA. Note that dominant-negative AMPK-α2 reduced significantly the number of SGs/cell and the total SG area/cell (**, $p<0.01$; One-way ANOVA for DEM-treated samples; results for the control plasmid served as reference).

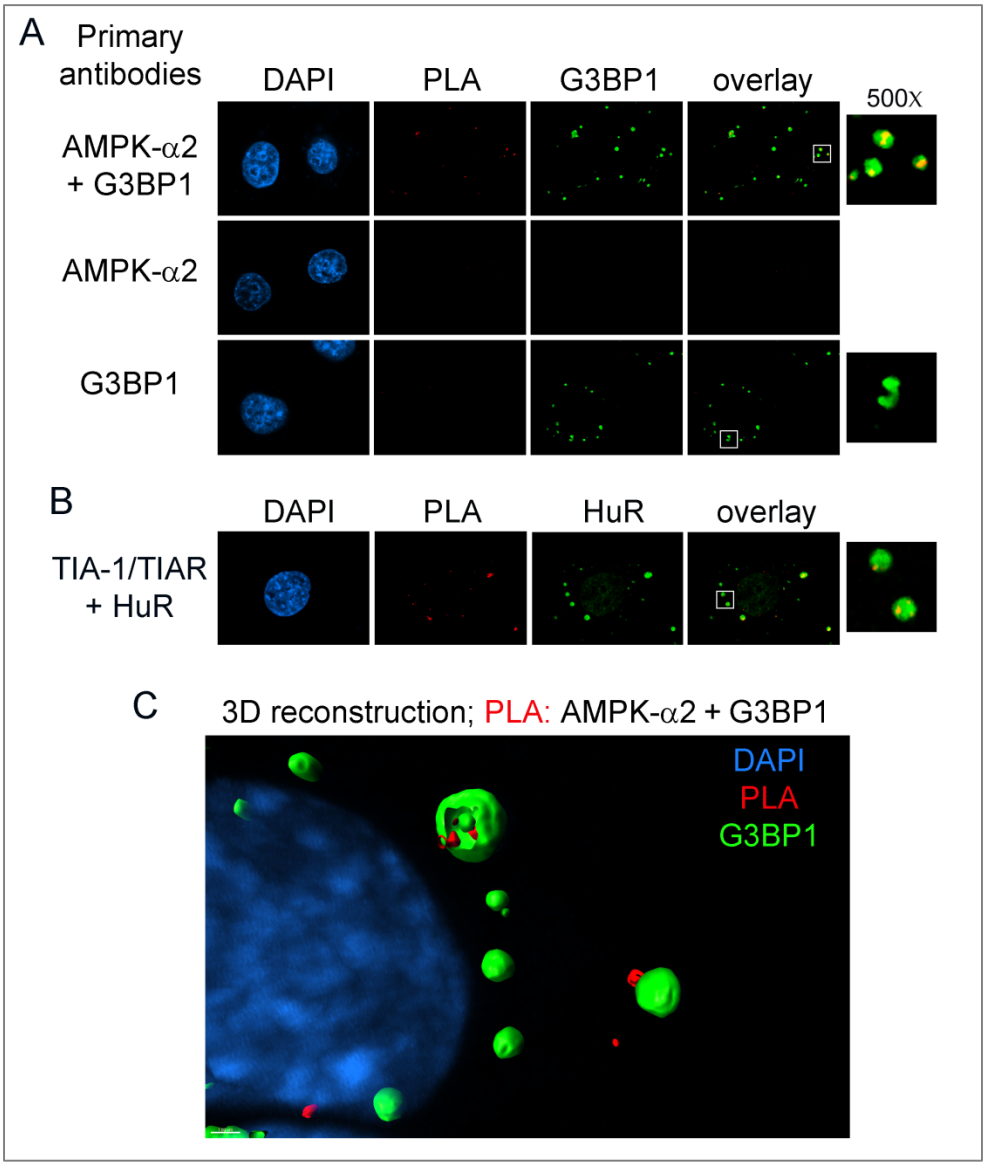

Fig. 9. AMPK-α2 interacts with G3BP1 in SGs. Cell were incubated with DEM as described for Fig. 1. Following the incubation with primary antibodies against AMPK-α2 and G3BP1, the proximity of both proteins was examined by PLA (red signal; Materials and methods). After PLA, secondary antibodies against G3BP1 demarcated SGs (green). (A) PLA reveals that AMPK-α2 and G3BP1 are in close contact; this association occurs at least in part in SGs. The magnified region displays SGs that show an interaction between AMPK-α2 and G3BP1. This association takes place only in a portion of the SG area. In control experiments one of the primary antibodies was omitted; all other steps were identical. All images were acquired at identical settings. Scale bar is 20µm. (B) HuR and TIA-1/TIAR provided a positive control for proteins interacting in SGs. (C) 3D-reconstruction defines regions where AMPK-α2 and G3BP1 are in close proximity (red). SGs were demarcated by immunolocalizations of G3BP1 (green). AMPK-α2 and G3BP1 associate in SGs, and additional contact sites are present in the cytoplasm. Scale bar is 1µm.

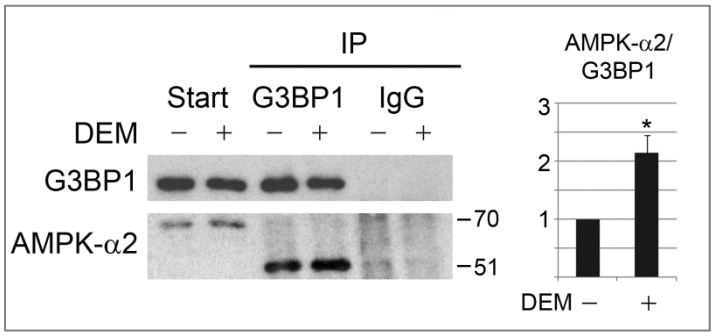

Fig. 10. AMPK-α2 and G3BP1 associate in control and stressed cells. HeLa cells were incubated with vehicle (EtOH) or DEM, and crude extracts were processed for immunoprecipitation (IP) with antibodies against G3BP1. Start indicates 20% of the starting material for the IP. Immunopurified material obtained for anti-G3BP1 and isotype control IgG were run side-by-side. The filter was first probed with antibodies against G3BP1, stripped and then reprobed with anti-AMPK-α2 antibodies. ECL signals obtained for G3BP1 and AMPK-α2 were quantified, the ratio AMPK-α2/G3BP1 was calculated and normalized to the control. The graph depicts the results of four independent experiments; it shows that the association of AMPK-α2 with G3BP1 significantly increased upon oxidative stress (Student's ttest).

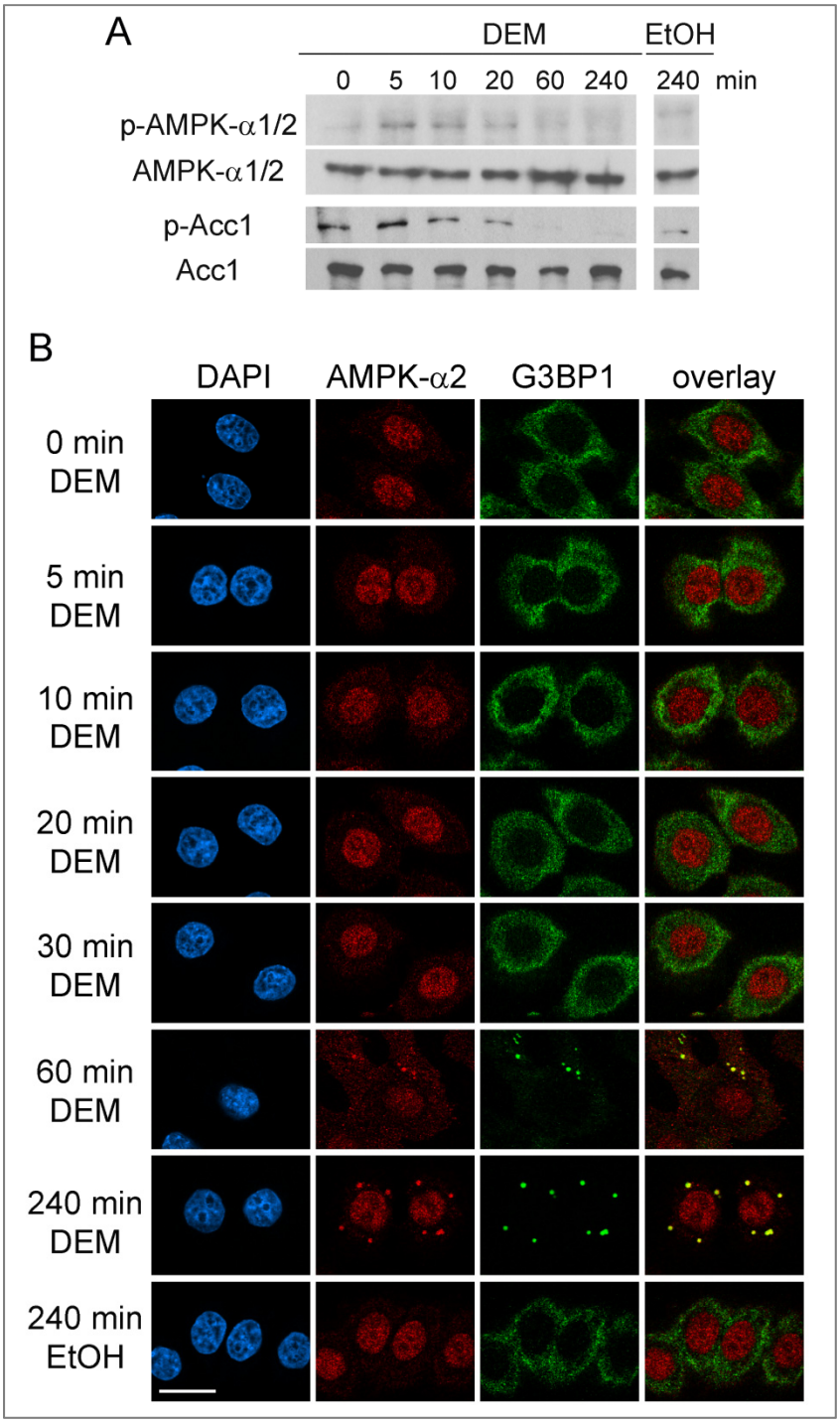

Fig. 11. AMPK activation precedes SG formation. HeLa cells were incubated with DEM for the time points indicated. (A) AMPK-α phosphorylation (p-AMPK-α1/2), total AMPK-α1/2, phosphorylated Acc1 (p-Acc1, Ser79) and total Acc1 were detected by Western blotting. Controls were incubated with the vehicle ethanol (EtOH). (B) The kinetics for SG formation was monitored by immunodetection of AMPK-α2 and G3BP1. SGs were formed after 60min incubation with DEM. They contained the marker G3BP1 and AMPK-α2.

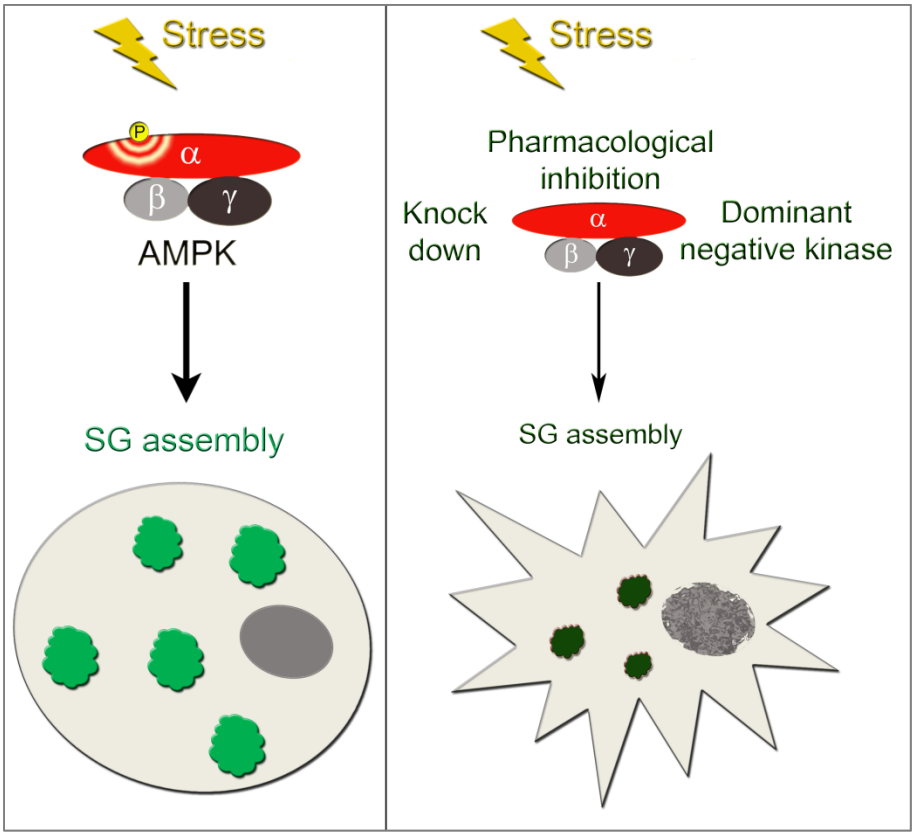

Fig. 12. Simplified model for the role of AMPK in SG biogenesis. Stress induces the transient activation of AMPK and the assembly of SGs (left panel). Reduced AMPK abundance or activation, achieved through pharmacological inhibition, kinase knockdown or a dominant-negative form of AMPK alters SG parameters, such as number or size.

Supplementary Figure and Table.

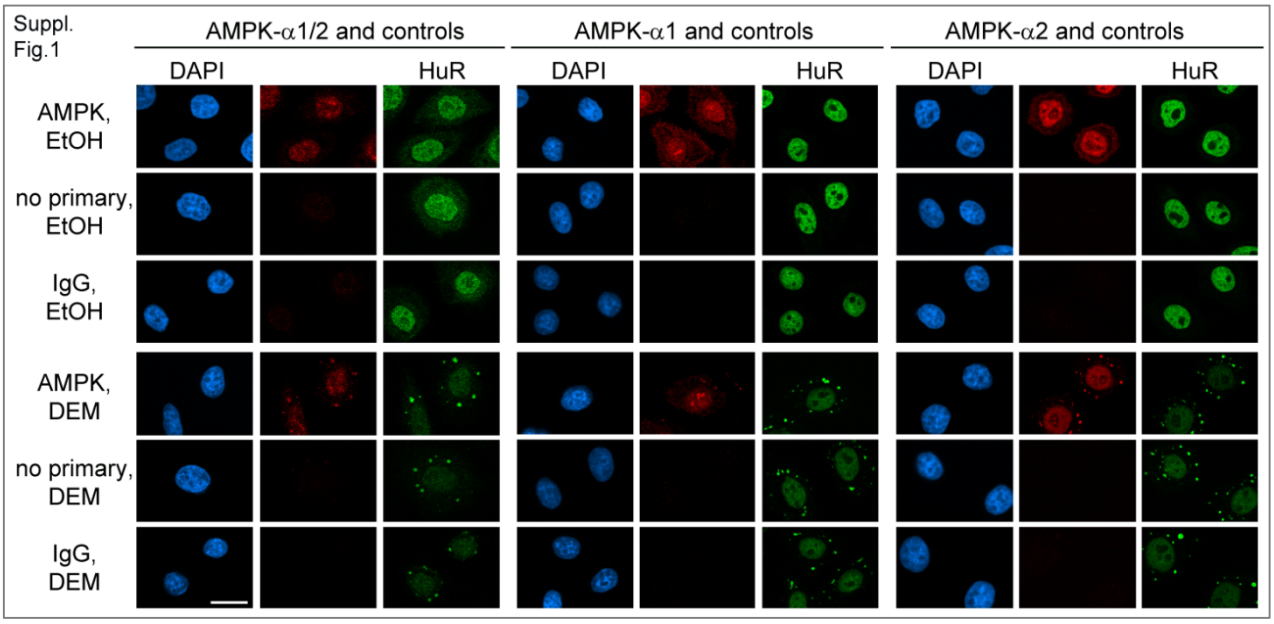

Fig. S1. Specificity of AMPK-α antibodies. The binding of AMPK-α1/2, AMPK-α1 and AMPK-α2, as well as secondary antibodies was examined for cells incubated with ethanol or DEM (Materials and methods). Control experiments were performed without primary antibodies or isotype-specific controls. SGs were identified with HuR; DNA was stained with DAPI. For each antibody, images were acquired at identical settings of the microscope. Scale bar is 20μm.

Table S1. Sequences of the shRNA constructs for AMPK-α knockdown. The hairpin loop is shown in lower case letters. All sequences were blasted against the human genome to confirm target recognition and rule out off-target effects.

Subunit targeted	**shRNA sequence**
AMPK-α1	GTG-ATT-AGC-CTT-TTG-AAA-C-cttcctgtca-G-TTT-CAA-AAG-GCT-AAT-CAC
AMPK-α1	GAC-TCG-GCC-CCA-TCC-TGA-A-cttcctgtca-T-TCA-GGA-TGG-GGC-CGA-GTC
AMPK-α2	AAT-GGA-ATA-TGT-GTC-TGG-AGG-cttcctgtca-CCT-CCA-GAC-ACA-TAT-TCC-ATT
AMPK-α2	AGA-TTG-TAT-GCA-GGT-CCT-GAA-cttcctgtca-TTC-AGG-ACC-TGC-ATA-CAA-TCT

References

[1] K. Arimoto, H. Fukuda, S. Imajoh-Ohmi, H. Saito, M. Takekawa, Formation of stress granules inhibits apoptosis by suppressing stress-responsive MAPK pathways, Nat. Cell Biol., 10 (2008) 1324-1332.

[2] N. Kedersha, P. Ivanov, P. Anderson, Stress granules and cell signaling: more than just a passing phase?, Trends Biochem. Sci., 38 (2013) 494-506.

[3] N.L. Kedersha, M. Gupta, W. Li, I. Miller, P. Anderson, RNA-binding proteins TIA-1 and TIAR link the phosphorylation of eIF-2 alpha to the assembly of mammalian stress granules, J. Cell Biol., 147 (1999) 1431-1442.

[4] N. Kedersha, P. Anderson, Mammalian stress granules and processing bodies, Methods Enzym., 431 (2007) 61-81.

[5] N. Kedersha, S. Chen, N. Gilks, W. Li, I.J. Miller, J. Stahl, P. Anderson, Evidence that ternary complex (eIF2-GTP-tRNA(i)(Met))-deficient preinitiation complexes are core constituents of mammalian stress granules, Mol. Biol. Cell, 13 (2002) 195-210.

[6] S. Mokas, J.R. Mills, C. Garreau, M.J. Fournier, F. Robert, P. Arya, R.J. Kaufman, J. Pelletier, R. Mazroui, Uncoupling stress granule assembly and translation initiation inhibition, Mol. Biol. Cell, 20 (2009) 2673-2683.

[7] N. Gilks, N. Kedersha, M. Ayodele, L. Shen, G. Stoecklin, L.M. Dember, P. Anderson, Stress granule assembly is mediated by prion-like aggregation of TIA-1, Mol. Biol. Cell, 15 (2004) 5383-5398.

[8] H. Tourriere, K. Chebli, L. Zekri, B. Courselaud, J.M. Blanchard, E. Bertrand, J. Tazi, The RasGAP-associated endoribonuclease G3BP assembles stress granules, J. Cell Biol., 160 (2003) 823-831.

[9] P. Anderson, N. Kedersha, RNA granules: post-transcriptional and epigenetic modulators of gene expression, Nat. Rev. Mol. Cell Biol., 10 (2009) 430-436.

[10] J.R. Buchan, J.H. Yoon, R. Parker, Stress-specific composition, assembly and kinetics of stress granules in Saccharomyces cerevisiae, J. Cell Sci., 124 (2011) 228-239.

[11] H. Mahboubi, M. Kodiha, U. Stochaj, Automated detection and quantification of granular cell compartments, Microsc. Microanal., 19 (2013) 617-628.

[12] N.P. Tsai, P.C. Ho, L.N. Wei, Regulation of stress granule dynamics by Grb7 and FAK signalling pathway, Embo J., 27 (2008) 715-726.

[13] N.P. Tsai, L.N. Wei, RhoA/ROCK1 signaling regulates stress granule formation and apoptosis, Cell Signal., 22 (2010) 668-675.

[14] K. Thedieck, B. Holzwarth, Mirja T. Prentzell, C. Boehlke, K. Kläsener, S. Ruf, Annika G. Sonntag, L. Maerz, S.-N. Grellscheid, E. Kremmer, R. Nitschke, E.W. Kuehn, Johan W. Jonker, Albert K. Groen, M. Reth, Michael N. Hall, R. Baumeister, Inhibition of mTORC1 by Astrin and Stress Granules Prevents Apoptosis in Cancer Cells, Cell, 154 (2013) 859-874.

[15] H. Mahboubi, U. Stochaj, Nucleoli and Stress Granules: Connecting Distant Relatives, Traffic, 15 (2014) 1179–1193.

[16] D.G. Hardie, F.A. Ross, S.A. Hawley, AMPK: a nutrient and energy sensor that maintains energy homeostasis, Nat. Rev. Mol. Cell Biol., 13 (2012) 251-262.

[17] D. Carling, C. Thornton, A. Woods, M.J. Sanders, AMP-activated protein kinase: new regulation, new roles? Biochem J., 445 (2012) 11-27.

[18] D.G. Hardie, D. Carling, S.J. Gamblin, AMP-activated protein kinase: also regulated by ADP? Trends Biochem. Sci., 36 (2011) 470-477.
[19] M. Kodiha, H. Mahboubi, U. Stochaj, Contributions of AMP kinase to the Pathogenesis of Type 2 Diabetes and Neurodegenerative Diseases., in: T. Farooqui, A.A. Farooqui (Eds.) Metabolic Syndrome and Neurological Disorders, Wiley-Blackwell, Place Published, 2013, pp. 363-381.
[20] J. Kim, M. Kundu, B. Viollet, K.L. Guan, AMPK and mTOR regulate autophagy through direct phosphorylation of Ulk1, Nat. Cell Biol., 13 (2011) 132-141.
[21] J. Liang, S.H. Shao, Z.-X. Xu, B. Hennessy, Z. Ding, M. Larrea, S. Kondo, D.J. Dumont, J.U. Gutterman, C.L. Walker, J.M. Slingerland, G.B. Mills, The energy sensing LKB1-AMPK pathway regulates p27kip1 phosphorylation mediating the decision to enter autophagy or apoptosis, Nat. Cell Biol., 9 (2007) 218-224.
[22] M.M. Mihaylova, R.J. Shaw, The AMPK signalling pathway coordinates cell growth, autophagy and metabolism, Nat. Cell Biol., 13 (2011) 1016-1023.
[23] V. Mirouse, L.L. Swick, N. Kazgan, D. St Johnston, J.E. Brenman, LKB1 and AMPK maintain epithelial cell polarity under energetic stress, J. Cell Biol., 177 (2007) 387-392.
[24] A. Nakano, H. Kato, T. Watanabe, K.D. Min, S. Yamazaki, Y. Asano, O. Seguchi, S. Higo, Y. Shintani, H. Asanuma, M. Asakura, T. Minamino, K. Kaibuchi, N. Mochizuki, M. Kitakaze, S. Takashima, AMPK controls the speed of microtubule polymerization and directional cell migration through CLIP-170 phosphorylation, Nat. Cell Biol., 12 (2010) 583-590.
[25] D.G. Hardie, S.A. Hawley, J.W. Scott, AMP-activated protein kinase – development of the energy sensor concept, J. Physiol., 574 (2006) 7-15.
[26] K.R. Hallows, P.F. Mount, N.M. Pastor-Soler, D.A. Power, Role of the energy sensor AMP-activated protein kinase in renal physiology and disease, Am J. Physiol. - Renal Physiol., 298 (2010) F1067-F1077.
[27] J.S. Oakhill, Z.P. Chen, J.W. Scott, R. Steel, L.A. Castelli, N. Ling, S.L. Macaulay, B.E. Kemp, beta-Subunit myristoylation is the gatekeeper for initiating metabolic stress sensing by AMP-activated protein kinase (AMPK), Proc. Natl. Acad. Sci. U. S. A., 107 (2010) 19237-19241.
[28] M.J. Sanders, P.O. Grondin, B.D. Hegarty, M.A. Snowden, D. Carling, Investigating the mechanism for AMP activation of the AMP-activated protein kinase cascade, Biochem. J., 403 (2007) 139-148.
[29] D.B. Shackelford, R.J. Shaw, The LKB1-AMPK pathway: metabolism and growth control in tumour suppression, Nat. Rev. Cancer, 9 (2009) 563-575.
[30] G.R. Steinberg, B.E. Kemp, AMPK in Health and Disease, Physiol. Rev., 89 (2009) 1025-1078.
[31] W. Lieberthal, M. Tang, L. Zhang, B. Viollet, V. Patel, J.S. Levine, Susceptibility to ATP depletion of primary proximal tubular cell cultures derived from mice lacking either the alpha1 or the alpha2 isoform of the catalytic domain of AMPK, BMC Nephrol., 14 (2013) 251.
[32] K.M. Neurath, M.P. Keough, T. Mikkelsen, K.P. Claffey, AMP-dependent protein kinase alpha 2 isoform promotes hypoxia-induced VEGF expression in human glioblastoma, Glia, 53 (2006) 733-743.
[33] T.-C. Ju, H.-M. Chen, J.-T. Lin, C.-P. Chang, W.-C. Chang, J.-J. Kang, C.-P. Sun, M.-H. Tao, P.-H. Tu, C. Chang, D.W. Dickson, Y. Chern, Nuclear translocation of AMPK-α1 potentiates striatal neurodegeneration in Huntington's disease, J. Cell Biol., (2011).

[34] Y.J. Liu, T.C. Ju, H.M. Chen, Y.S. Jang, L.M. Lee, H.L. Lai, H.C. Tai, J.M. Fang, Y.L. Lin, P.H. Tu, Y. Chern, Activation of AMP- activated protein kinase alpha1 mediates mislocalization of TDP-43 in amyotrophic lateral sclerosis, Hum. Mol. Genet., (2014).
[35] S.J. Parker, J. Meyerowitz, J.L. James, J.R. Liddell, P.J. Crouch, K.M. Kanninen, A.R. White, Endogenous TDP-43 localized to stress granules can subsequently form protein aggregates, Neurochem. Int., 60 (2012) 415-424.
[36] R. Mazroui, R. Sukarieh, M.E. Bordeleau, R.J. Kaufman, P. Northcote, J. Tanaka, I. Gallouzi, J. Pelletier, Inhibition of ribosome recruitment induces stress granule formation independently of eukaryotic initiation factor 2alpha phosphorylation, Mol. Biol. Cell, 17 (2006) 4212-4219.
[37] M. Kodiha, J.G. Rassi, C.M. Brown, U. Stochaj, Localization of AMP kinase is regulated by stress, cell density, and signaling through the MEK→ERK1/2 pathway, Am. J. Physiol. - Cell Physiol., 293 (2007) C1427-1436.
[38] H. Mahboubi, E. Seganathy, D. Kong, U. Stochaj, Identification of Novel Stress Granule Components That Are Involved in Nuclear Transport, PLoS One, 8 (2013) e68356.
[39] H. Mahboubi, R. Barisé , U. Stochaj, Data in support of 5'-AMP-kinase regulates the biogenesis of stress granules, Data in Brief, (2015).
[40] J. Mu, J.T. Brozinick Jr, O. Valladares, M. Bucan, M.J. Birnbaum, A Role for AMP-Activated Protein Kinase in Contraction- and Hypoxia-Regulated Glucose Transport in Skeletal Muscle, Mol. Cell, 7 (2001) 1085-1094.
[41] I. Baaklini, M.J. Wong, C. Hantouche, Y. Patel, A. Shrier, J.C. Young, The DNAJA2 substrate release mechanism is essential for chaperone-mediated folding, J. Biol. Chem., 287 (2012) 41939-41954.
[42] M. Kodiha, D. Tran, C. Qian, A. Morogan, J.F. Presley, C.M. Brown, U. Stochaj, Oxidative stress mislocalizes and retains transport factor importin-alpha and nucleoporins Nup153 and Nup88 in nuclei where they generate high molecular mass complexes, Biochim. Biophys. Acta, 1783 (2008) 405-418.
[43] N. Crampton, M. Kodiha, S. Shrivastava, R. Umar, U. Stochaj, Oxidative stress inhibits nuclear protein export by multiple mechanisms that target FG nucleoporins and Crm1, Mol. Biol. Cell, 20 (2009) 5106-5116.
[44] D. Milan, J.-T. Jeon, C. Looft, V. Amarger, A. Robic, M. Thelander, C. Rogel-Gaillard, S. Paul, N. Iannuccelli, L. Rask, H. Ronne, K. Lundström, N. Reinsch, J. Gellin, E. Kalm, P.L. Roy, P. Chardon, L. Andersson, A Mutation in PRKAG3 Associated with Excess Glycogen Content in Pig Skeletal Muscle, Science, 288 (2000) 1248-1251.
[45] G. Zhou, R. Myers, Y. Li, Y. Chen, X. Shen, J. Fenyk-Melody, M. Wu, J. Ventre, T. Doebber, N. Fujii, N. Musi, M.F. Hirshman, L.J. Goodyear, D.E. Moller, Role of AMP-activated protein kinase in mechanism of metformin action, J Clin. Investig., 108 (2001) 1167-1174.
[46] S. Hofmann, V. Cherkasova, P. Bankhead, B. Bukau, G. Stoecklin, Translation suppression promotes stress granule formation and cell survival in response to cold shock, Mol. Biol. Cell, 23 (2012) 3786-3800.
[47] J. Jin, T.D. Mullen, Q. Hou, J. Bielawski, A. Bielawska, X. Zhang, L.M. Obeid, Y.A. Hannun, Y.T. Hsu, AMPK inhibitor Compound C stimulates ceramide production and promotes Bax redistribution and apoptosis in MCF7 breast carcinoma cells, J. Lipid Res., 50 (2009) 2389-2397.

[48] X. Liu, R.R. Chhipa, I. Nakano, B. Dasgupta, The AMPK inhibitor Compound C is a potent AMPK-independent anti-glioma agent, Mol. Cancer Ther., (2014).
[49] S. Saito, A. Furuno, J. Sakurai, H.R. Park, K. Shin-ya, A. Tomida, Compound C prevents the unfolded protein response during glucose deprivation through a mechanism independent of AMPK and BMP signaling, PLoS One, 7 (2012) e45845.
[50] L. Tangeman, C.N. Wyatt, T.L. Brown, Knockdown of AMP-activated protein kinase alpha 1 and alpha 2 catalytic subunits, J. RNAi Gene Silencing, 8 (2012) 470-478.
[51] H. Xu, Y. Zhou, K.A. Coughlan, Y. Ding, S. Wang, Y. Wu, P. Song, M.-H. Zou, AMPKα1 deficiency promotes cellular proliferation and DNA damage via p21 reduction in mouse embryonic fibroblasts, Biochim. Biophys. Acta, 1853 (2015) 65-73.
[52] J.A. Collins, C.A. Schandi, K.K. Young, J. Vesely, M.C. Willingham, Major DNA fragmentation is a late event in apoptosis, J. Histochem. Cytochem., 45 (1997) 923-934.
[53] P. David Gerecht, M. Taylor, J. Port, Intracellular localization and interaction of mRNA binding proteins as detected by FRET, BMC Cell Biol., 11 (2010) 69.
[54] N. Kedersha, G. Stoecklin, M. Ayodele, P. Yacono, J. Lykke-Andersen, M.J. Fritzler, D. Scheuner, R.J. Kaufman, D.E. Golan, P. Anderson, Stress granules and processing bodies are dynamically linked sites of mRNP remodeling, J. Cell Biol., 169 (2005) 871-884.
[55] D. Chanda, S.-J. Kim, I.-K. Lee, M. Shong, H.-S. Choi, Sodium arsenite induces orphan nuclear receptor SHP gene expression via AMP-activated protein kinase to inhibit gluconeogenic enzyme gene expression, Am. J. Physiol. Endocrinol. Metab., 295 (2008) E368-E379.